

A Precise Gait Phase Detection Based on High-Frequency Vibration on Lower Limbs

Shuhei Kadoya¹, Naohisa Nagaya², Masashi Konyo² and Satoshi Tadokoro²

Abstract—A novel gait phase detection method that can extract the timing of foot contact conditions (Heel Strike and Toe Off) by a single piezo film sensor attached on each leg is proposed. We focused on the occurrence of high-frequency vibrations (> 100 Hz) in the beginning and the end of stance phases during gait. After the features of vibration waveforms during gait were confirmed, we proposed the phase detection method. The optimal parameters were investigated to detect the phases robustly despite the walking speed and the shoe types. Experimental results showed that the detected ground contact events had high accuracy of timing. Finally, we confirmed the feasibility with the prototype wearable device in usual environments.

I. INTRODUCTION

Gait phases are functional units segmented with the relevant timing of motions in a gait cycle. Detection methods of the gait phases are fundamental not only for clinical gait analysis, but also for future engineering applications such as a robotic walking support system and a ubiquitous health monitoring system.

A gait cycle is divided into two primary phases, the stance phase and the swing phase. The stance phase can be subdivided into the detailed gait phases with the relevant timings, Heel Strike (HS), Heel Off (HO), and Toe Off (TO), observed with the ground contact condition at the heel and toe as shown in Fig. 1. In physical medicine and rehabilitation fields, gait phases are defined by the combination of timings of HS, HO, and TO in the both legs [1]. In engineering fields, the gait phase detection is also necessary for a gait support system and human-machine interfaces synchronized with gait motion. For example, a walking assistance system requires a distinction of the stance phase and the swing phase for controlling assistive force so that the detection of HS and TO is necessary. In a study of a personal navigation system, detecting the timing of the Mid Stance, in which foot's velocity becomes zero, performed precise estimation of trajectories of a human locomotor equipped with inertial measurement unit (IMU) [2], [3]. In studies of haptic display for gait feeling [4], [5], detection of HS is also important for producing stimulation on foot in synchronized with the ground contacts. In this sense, detecting exact timings of

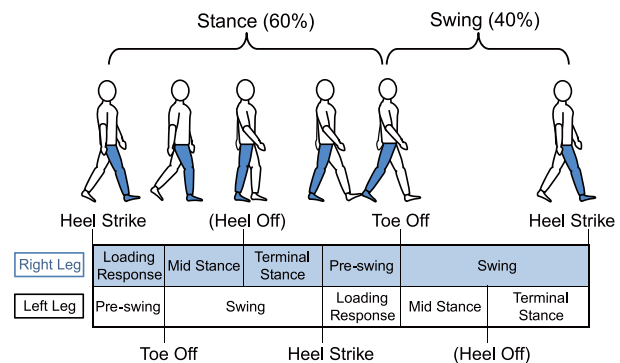


Fig. 1. Common definition of gait phases

HS, HO and TO is the fundamental procedure for the gait analysis and the gait support systems.

Conventionally, there are several approaches for the gait phase detection. In basic studies, many commercial gait analysis systems are available, involving force plates and pressure distribution sensors (a sheet type or an insole type) for detecting foot contact conditions. On the other hand, for aiming practical use in daily life, there are mainly two approaches: a pressure-sensing type and an IMU type.

Pressure-sensing types use pressures sensors such as pressure-sensitive rubber sensors, air pressure sensors, or strain gauges, installed to the outside/inside of the shoes. For example, Kong et al. [6] developed a smart shoe that can measure ground contact forces (GCF), embedded with air bladders and air pressure sensors in the sole. A fuzzy logic estimator based on pressure patterns distinguished the gait phases. Chen et al. [7] proposed a shoe-integrated system, which consists of an IMU and flexible pressure sensors mounted on the insole, for human abnormal gait detection. While the pressure-sensing types can detect relatively precise timing of HS, HO, and TO because they measure contact pressure at the foot directly, available shoes are limited. An insole type can be applied for various kinds of shoes but not for all, especially for a bare foot.

IMU types, consisting of multi-dimensional accelerometers and gyroscopes, are attached to legs or shoes and estimate gait motions and contact conditions. Although a shoe-mounted IMU [8]–[13] can detect contact condition with relatively high accuracy, it has the same limitation of attachment on shoes as well as the pressure-sensing type. Leg-mounted IMU types [14]–[16] are available for any footwear. They detect gait phases by attaching multiple IMUs on several parts of legs such as thighs and shanks.

*This work was not supported by any organization

¹S. Kadoya is with the Department of Mechanical and Aerospace Engineering, School of Engineering, Tohoku University, 6-6-01 Aramaki Aza Aoba, Aoba-ku, Sendai, Miyagi, 980-8579, Japan kadoya@rm.is.tohoku.ac.jp

²N. Nagaya, M. Konyo, and S. Tadokoro with the Graduate School of Information Sciences, Tohoku University, 6-6-01 Aramaki Aza Aoba, Aoba-ku, Sendai, Miyagi, 980-8579, Japan nagaya, konyo, tadokoro@rm.is.tohoku.ac.jp

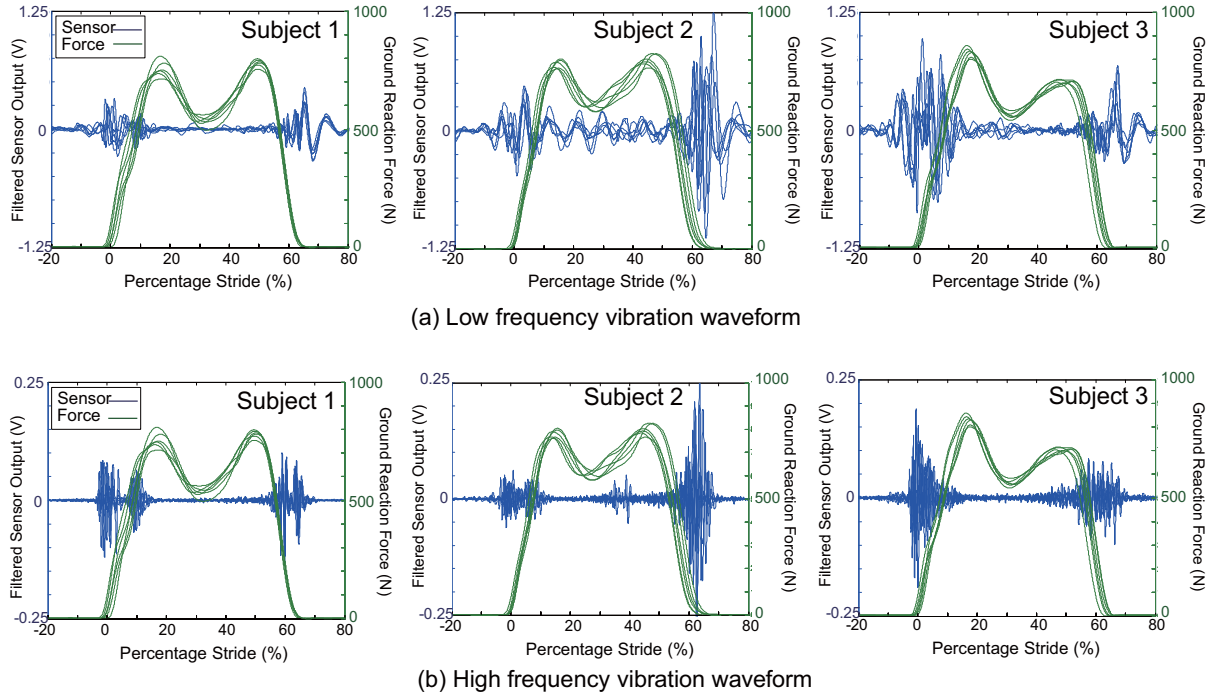


Fig. 2. The example of the vibration waveform for a) low frequency and b) high frequency for 3 different subjects

A drawback of the leg-mounted IMU types might be lower accuracy of the phase detection than the pressure-sensing types. Mansfield et al. [16] reported that HS detection had approximately 150 ms delay with their IMU-based method. In addition, putting multiple IMUs on legs takes time and may not be suitable for use in daily life.

In this paper, we propose a novel gait phase detection methods that can extract the timing of foot contact conditions (HS and TO) by a single simple sensor attached on each leg regardless of footwear types. Comparing with the conventional leg-mounted IMU type, the method proposed has high accuracy in detection time for HS and TO. Our new viewpoint is the occurrence of high-frequency vibrations (> 100 Hz) in the beginning and the end of stance phases during gait. As far as the authors' knowledge, there is no literature focusing on such high-frequency vibration propagating on legs for the gait phase detection. In this paper, we confirm that the high-frequency vibrations achieved by piezofilm sensors attached on ankles have peaks near HS and TO in the stance phases. A stance phase detection method is proposed based on the feature of the observed vibration waveforms. Then, we explore the optimal parameters in the proposed method for detecting the gait phases robustly despite the walking speed and the shoe types. Finally, time accuracy of the detected phases is evaluated.

II. MEASURING METHOD AND CHARACTERISTIC OF VIBRATION

A. Measuring Method

In this study, vibrations during gait were measured using a piezo film sensor (SDT1-028K, Measurement Specialties,

Inc.) which can measure in a wide frequency range (up to 50 kHz) and has a flat frequency response. The piezo film sensor converts its deformation to voltage. Output signals are amplified by an amplifier (PA-20DB, Tokyo Sensor Co., Ltd.) and filtered with an analog bandpass filter (6-1600 Hz).

As reference data for true timing of HS and TO, ground reaction forces were measured by dual-belt treadmill with force plates (ITR5018, Bertec Corp). The treadmill can acquire separate ground reaction forces for both feet and change speed from 0 km/h to 20 km/h.

The piezo film sensor was attached on the ankle (lower tibia around Medial malleolus) of each leg. All data were recorded by a multi-channel 16 bits datalogger (NR-600, Keyence Co., Ltd) at the sampling frequency of 5 kHz.

B. Characteristic

Typical features of generated vibration at the legs during gait are investigated in this section. Especially, we discuss the differences between high and low frequency components in the timing of ground contacts at the stance phase.

Fig. 2 shows the 5 step samples of vibration waveform for three subjects and ground reaction forces are also plotted as a reference of gait phases. The top graphs (a) show the low frequency components, which are filtered with a band-pass filter (5th-order Butterworth filter; cut-off frequency 10–100 Hz), and the bottom (b) shows the high frequency components, which are filtered with a band-pass filter (5th-order Butterworth filter; cut-off frequency 50–150 Hz). The horizontal-axis shows gait cycle in percentage stride of -20% to 80% , where 0% represents a heel strike and 100% is the next heel strike. The left vertical axis is for the filtered

sensor outputs, and right vertical-axis is for the ground reaction force.

The vibration peaks appear near heel strike and toe off for both the low frequency and the high frequency. So it indicates that using vibration is possible to measure HS and TO. The high frequency appears in the short term at HS and TO comparing with the low frequency. It indicates high frequency can determine the accurate timing of HS and TO. However, the high frequency components are not so confident to detect the contact events because sometimes it have an unique shape depending subjects, for example, two peaks appear near the same event (Subject 1) or several peaks appear between HS and TO (Subject 2). The low frequency, on the other hand, less unique shape and has large peaks only near heel strike and toe off that makes easier to detect heel strike and toe off. Therefore, it is the best to use the low frequency components for the indication of approximate timing of heel strike and toe off, and the high frequency for determining more specific timing.

III. HEEL STRIKE AND TOE OFF DETECTION

A. Phase Detection Method Proposed

In this section, a more specific phase detection method is described.

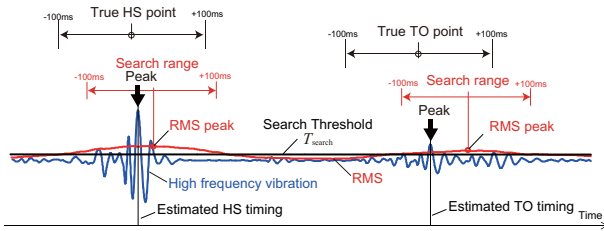


Fig. 3. Proposed gait phase detection method

For finding approximate timing of the contact events stably, the low frequency components are converted to RMS (root mean square), which makes signals much smooth, and then used to narrow down the possible detection term for finding peaks of the high frequency at the ground contact events. The detail of detection processes is given as follows:

1. Normalization: an acquired sensor signal is filtered with the bandpass of 10–150 Hz, then normalized with the maximum value of the filtered data.
2. RMS: Determine the RMS of the normalized data. (The applied RMS sample number N is optimized in later section)
3. Noise Threshold: Determine the mean of the absolute value of the normalized data in the step 1 from the first 5 steps, which are assumed as a calibration process in a practical use. This value becomes the threshold T_{noise} for removing small noise of the signals.
4. Mean RMS: Determine the mean of the RMS that exceeds the T_{noise} .
5. Search Threshold: Multiply the Mean RMS with the weight m . This value becomes the threshold T_{search} for finding possible range of the ground contact events. (The weight m is optimized in the later section)

6. Max RMS: Find the maximum of RMS that exceeds the threshold T_{range}
7. Finding Peaks: Find peaks of the high frequency component in the range of ± 100 ms from the Max RMS point in the previous step. (100 ms is about 10% of the gait cycle in 4 km/h walking speed)

To optimize this method, the best RMS sample number N and threshold weight m should be determined. The optimization is conducted in the next section.

B. Optimization RMS Samples and Threshold Statement

The RMS sample number N and search threshold weight m are needed to optimized as described in the previous section. RMS is applied to generalize the trend of the peak of the low frequency components. The sample number N should be chosen to extract the approximate range of the ground contact events. More sample number will generalize more, but too many sample number will eliminate necessary information. After preliminary investigation, we selected possible range of RMS sampling numbers as follows: 600, 900, and 1200.

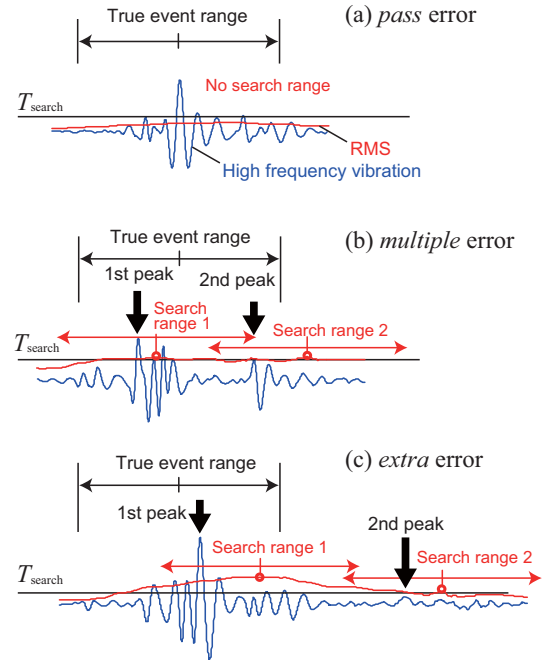


Fig. 4. Definition of three types of error.

The weight m is aimed to adjust the search threshold T_{search} for extracting possible ranges of the contact events from the RMS curve. If T_{search} is too large, no possible range to be searched is found. If T_{search} is too small, many wrong search area could be found. After preliminary investigation, we found the possible value is around 0.50 so that we selected m from 0.40 to 0.60 for the optimization.

Investigating parameters for the optimization are summarized as follows:

- N : 600, 900, 1200 points
- m : 0.40, 0.45, 0.50, 0.55, 0.60

C. Detection Performance Metrics

To evaluate the detection performance, we defined the possible case of errors as follows:

- *pass* error: No search range is achieved because the RMS does not exceed the threshold T_{search} near the contact events. Fig. 4 (a) shows an example of *pass* error, where the RMS near the event does not exceed the threshold.
- *multiple* error: Multiple events are detected within the ± 100 ms range of the true event because RMS has multiple peaks and exceeds the threshold T_{Search} more than twice. Fig. 4 (b) shows an example of *multiple* error, where the RMS exceeds the threshold twice in the range of the event, and another peak is detected.
- *extra* error: Extra events are detected out of the ± 100 ms range of the true event. The reason is same as *multiple* error, but one or more peaks are detected out of the event range. Fig. 4 (c) shows an example of *extra* error, where the RMS exceeds threshold twice, and one peak is out of the range of the event.

The successful detection is defined as a rate of detection occurrence that does not contain any errors defined above.

D. Experimental Data Set

Experimental data set for optimizing the phase detection method were achieved by conducting the measurements of vibrations with various footwear and walking speeds.

Six subjects (all male in their age from 22 to 23 years old) walked on the treadmill for 30 seconds, and ground reaction forces were measured as a reference. Walking speeds were 3, 4, 5 [km/h], which were controlled by the treadmill constantly. It is known that typical walking speed for an adult is 4 km/h.

Three kinds of footwear were selected as follows:

- Bare foot: wear nothing
- Sandal: a simple slip-in sandal, which only instep is fixed by two belts
- Running shoes: a running shoes with shock absorber in the sole

E. Optimization Results

We analysed the successful detection rate for the experimental data set by changing the detection parameters described in optimization.

First, we compare the result for three kinds of footwear at walking speed of 4 km/h, which is the usual walking speed. Results of the successful detection rate for each condition are shown in Fig. 5. For the RMS sample number N , the $N = 900$ has relatively higher score for the bare foot and the running shoes except for the sandal. For the threshold weight m , $m = 0.5$ has relatively higher score rate on average if focusing on the condition of $N = 900$. Therefore, we assumed that a possible combination of optimized parameters is $N = 900$ and $m = 0.5$.

Second, we verified the robustness of the determined parameters against the walking speeds. Fig. 6 shows the

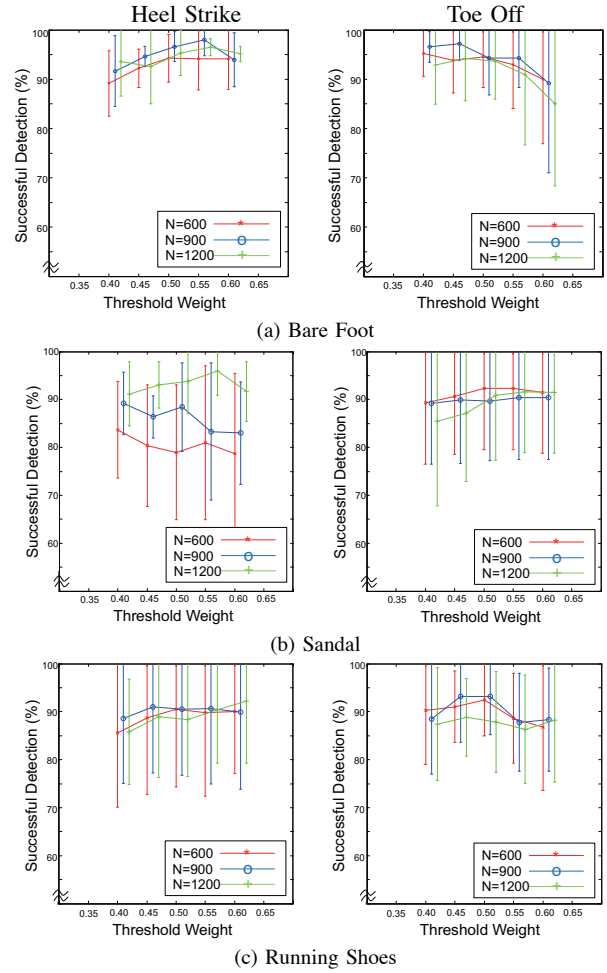


Fig. 5. Successful detection result of the shoes for all given RMS samples and threshold weight at walking speed of 4 km/h.

successful detection rate averaged from all the subject in the different walking speed on each footwear. In the most cases, the averaged detection rates are over 90. Therefore, we concluded that the assumed optimal parameters are reasonable enough.

IV. ACCURACY OF TIMING

In this section, the accuracy of detection timing achieved in the previous section is discussed.

To verify the effect of the high frequency components (filtered with 50 –150 Hz band pass filter), we compare the difference in detection timing with lower frequency components, which are assumed that the band pass filter for the sensor output is set to lower frequency range in 10 – 100 Hz.

Fig.7 shows the histograms of detected timing errors in comparison of the frequency range of the band pass filter; upper red bars represent the errors of the high frequency range filter and lower blue bars represent that of the low frequency range. The left side is the timing error about HS and the right side is TO for three kinds of footwear. All the experimental conditions are in the walking speed of 4

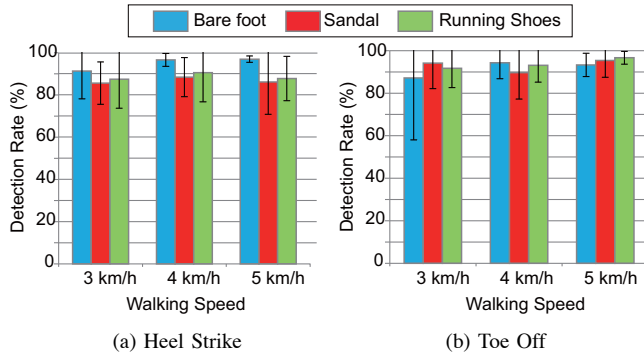


Fig. 6. Successful detection for all footwears and walking speeded at 900 RMS points and 0.5 threshold weight

km/h. Note that we excluded the timing error out of ± 100 [ms] range from the histogram and counted them as the out of range (OR) error. The observed OR error rate for the high frequency estimation were 0.91% for HS in the sandal and 3.23% for HS in the running shoes. No OR error was observed in other conditions.

For the timing error of HS, the histograms clearly show that the high frequency range has sharp and accurate score near zero on each kind of footwear comparing with the low frequency range. As for TO, while the detection errors spread in relatively wide range, the occurrence rate of appearing near zero for the high frequency range is higher than that of the low frequency range. There is a tendency that the detection timing with the high frequency range occurs in advance of the event timing, and that of the low frequency range has a delay from the event timing.

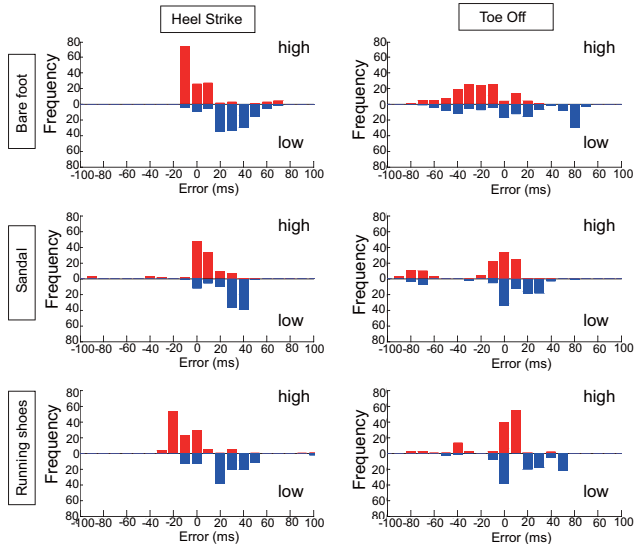


Fig. 7. Time error for successful detections (over 100 ms is excluded) with shoes at walking speed of 4 km/h for all subjects. The results are bare foot, sandal, and shoes from the top. Upper part of histogram shows the result of high frequency and lower part of histogram shows the result of low frequency.

These results demonstrate that the high frequency vibra-

tion has the high potential to extract the accurate timing of the contact events during gait. If we compare the accuracy of the proposed method with the best conventional studies, which use IMU sensor mounted on foot (shoes) with sophisticated algorithms [12], the timing of accuracy in this study is comparable to them. The mean and the standard deviation of timing errors were -7.64 ± 19.65 [ms] for HS and -4.86 ± 23.10 [ms] for TO in the condition of the running shoes. Mannini et al. [12] reported that their estimation errors were 8 ± 32 [ms] for HS and 11 ± 15 [ms] for TO in the condition of walking with the HMM-based method.

If we say the difference of our method, our sensing algorithm is very simple and the piezo film sensor is able to be attached on legs except for feet or shoes. The successful detection rates in Fig. 6, however, is still lower than the conventional methods (about 99%). In this sense, we may be able to find the model-based approach or the combination with IMUs to estimate the gait phase certainly.

V. FEASIBILITY TEST IN USUAL ENVIRONMENT

The two subjects (both male in their age from 23 to 24 years old) walked on the carpet floor with elliptic orbit which contains turning motion (to the left), and the same data as previous experiment was recorded with the prototype device. This device can be carried, and acquire vibration data with piezo film sensor and ground reaction force, as the reference data, with FlexiForce (FF-SET-A2014-25-8: Nitta co.,Ltd) placed underneath the heel and foot thumb. The pressure of the heel FlexiForce will begin to rise when HS occurs and the pressure of toe off will end to fall when TO occurs.

The result is shown in Fig. 8. The red line represents heel pressure, blue represents toe pressure, and the black line represents a detection by using the detection method. The black line appears near HS and TO precisely that indicates the method successfully detected HS and TO in the usual environment. Even with mixing of turning motion during walking, it still detected HS and TO successfully. Therefore this method has high usability.

VI. CONCLUSIONS

A novel gait phase detection method that can extract the timing of foot contact conditions (Heel Strike and Toe Off) by a single piezo film sensor attached on each leg is proposed. We focused on the occurrence of high-frequency vibrations (> 100 Hz) in the beginning and the end of stance phases during gait. The method is proposed based on the feature of observed vibration waveforms. We investigate the optimal parameters for detecting the gait phases robustly despite the walking speed and the shoe types. Experimental results showed that the high-frequency-vibration-based method had high accuracy of timing, comparing with the low frequency-based methods. Finally, we confirmed the feasibility of the proposed method with the prototype wearable device in usual environments.

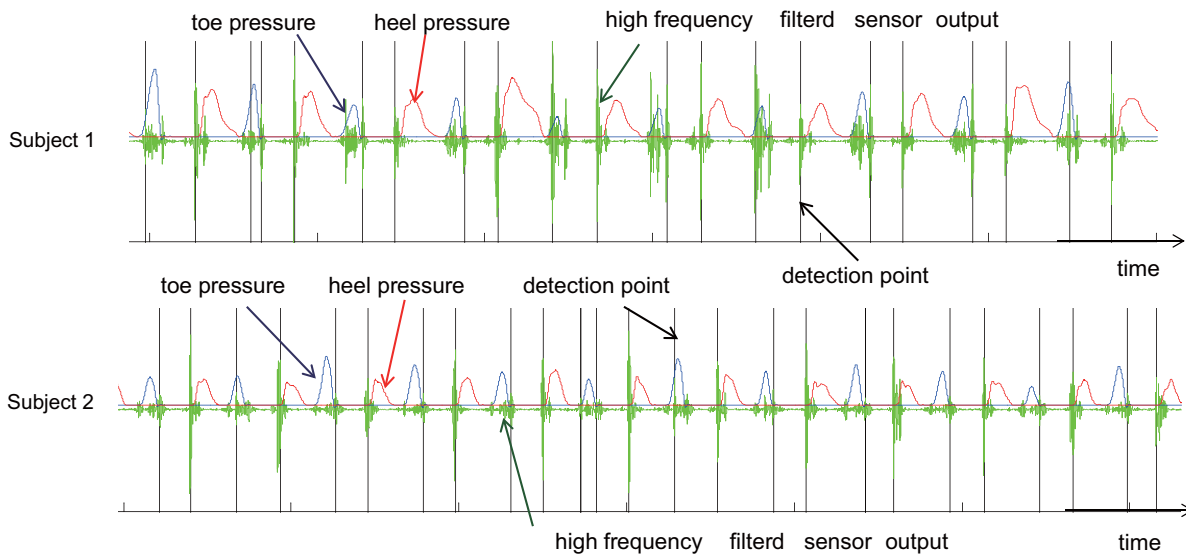


Fig. 8. Feasibility test for free walking on the carpet floor with a wearable prototype system.

The proposed method is so simple that it can be applied for gait analysis in daily life for many purposes such as robotic motion support systems and health monitoring systems.

ACKNOWLEDGMENT

This research was partially supported by the Cabinet Office, Government of Japan through its "Funding Program for Next Generation World-Leading Researchers."

REFERENCES

- [1] Observational gait analysis, Los Amigos Research and Education Institute, Downey, CA, 2001.
- [2] O. Bebek, M. a Suster, S. Rajgopal, M. J. Fu, M. C. Cavusoglu, D. J. Young, M. Mehregany, a J. van den Bogert, and C. H. Mastrangelo, Personal navigation via shoe mounted inertial measurement units, 2010 IEEE/RSJ International Conference on Intelligent Robots and Systems, no. i, pp. 1052–1058, Oct. 2010.
- [3] J. Borenstein, L. Ojeda, and S. Kwanmuang, Heuristic Reduction of Gyro Drift for Personnel Tracking Systems, *Journal of Navigation*, vol. 62, no. 01, p. 41, 2009.
- [4] Y. Visell, F. Fontana, B. L. Giordano, R. Nordahl, S. Serafin, and R. Bresin, Sound design and perception in walking interactions, *International Journal of Human-Computer Studies*, vol. 67, no. 11, pp. 947–959, Nov. 2009.
- [5] S. Papetti, F. Fontana, M. Civolani, A. Berrezag, and V. Hayward, Audio-tactile display of ground properties using interactive shoes, *Haptic and Audio Interaction Design*, pages 117–128, 2010.
- [6] K. Kong and M. Tomizuka, Smooth and continuous human gait phase detection based on foot pressure patterns, 2008 IEEE International Conference on Robotics and Automation, pp. 3678–3683, May 2008.
- [7] M. Chen, B. Huang, K. Lee, and Y. Xu, An intelligent shoe-integrated system for plantar pressure measurement, *Robotics and Biomimetics*, ROBIO'06, pp. 416–421, 2006.
- [8] K. Aminian, B. Najafi, C. Bula, P. F. Leyvraz, and P. Robert, Spatio-temporal parameters of gait measured by an ambulatory system using miniature gyroscopes, *Journal of biomechanics*, vol. 35, no. 5, pp. 689–99, May 2002.
- [9] S. J. Morris and J. A. Paradiso, A Compact Wearable Sensor Package for Clinical Gait Monitoring, vol. 1, no. 1, pp. 7–15, 2003.
- [10] A. M. Sabatini, C. Martelloni, S. Scapellato, and F. Cavallo, Assessment of walking features from foot inertial sensing, *IEEE transactions on bio-medical engineering*, vol. 52, no. 3, pp. 486–494, Mar. 2005.
- [11] L. Tao, Y. Inoue, K. Shibata, and H. Morioka, Development of wearable sensor combinations for human lower extremity motion analysis, *Proceedings 2006 IEEE International Conference on Robotics and Automation*, 2006. ICRA 2006., no. May, pp. 1655–1660, 2006.
- [12] A. Mannini and A. M. Sabatini, Gait phase detection and discrimination between walking-jogging activities using hidden Markov models applied to foot motion data from a gyroscope, *Gait and posture*, vol. 36, no. 4, pp. 657–61, Sep. 2012.
- [13] I. P. Pappas, M. R. Popovic, T. Keller, V. Dietz, and M. Morari, A reliable gait phase detection system, *IEEE transactions on neural systems and rehabilitation engineering : a publication of the IEEE Engineering in Medicine and Biology Society*, vol. 9, no. 2, pp. 113–25, Jun. 2001.
- [14] A. T. M. Willemsen, F. Bloemhof, and H. B. Boom, Automatic stance-swing phase detection from accelerometer data for peroneal nerve stimulation, *IEEE transactions on bio-medical engineering*, vol. 37, no. 12, pp. 1201–1208, Dec. 1990.
- [15] K. Tong and M. H. Granat, A practical gait analysis system using gyroscopes, *Medical engineering and physics*, vol. 21, no. 2, pp. 87–94, Mar. 1999.
- [16] A. Mansfield and G. M. Lyons, The use of accelerometry to detect heel contact events for use as a sensor in FES assisted walking, *Medical Engineering and Physics*, vol. 25, no. 10, pp. 879–885, Dec. 2003.
- [17] D. Kotiadis, H. J. Hermens, and P. H. Veltink, Inertial Gait Phase Detection for control of a drop foot stimulator Inertial sensing for gait phase detection, *Medical engineering and physics*, vol. 32, no. 4, pp. 287–297, May 2010.